

Research on Random Redundant Multi-Carrier Phase Code Signal against ISRJ Based on MIMO Radar

Ji Li¹, Qian Deng¹, Jianping Ou², and Wei Wang^{1, *}

Abstract—For the principle that intermittent sampling and repeater jamming (ISRJ) is obtained by discontinuous sampling of radar signal in time domain, a novel random redundancy (RR) waveform based on multiple input multiple output (MIMO) radar and multi-carrier phase code (MCPC) radar signal is proposed, namely RR-MCPC signal. From the point of waveform design, chaotic sequences are used to encode each chip in time domain for the signal with a multi-carrier phase code multiphase coding structure. Moreover, some chips are randomly arranged with equal amount of redundant coding in time-frequency domain. In MIMO radar, the subcarriers of radar signal are divided into multiple channels for transmission, and then the received signal is processed in each channel. Ensure that the intermittent sampling, whether in time domain or frequency domain, will sample redundant information in a channel. So it cannot match the matched filter. Therefore, the RR processing makes the signal have the characteristics of anti-ISRJ, which can availably restrain the interference of ISRJ false target. The results show that the signal-jamming ratio (SJR) improvement factor of RR-MCPC signal after pulse compression is optimized by 2.47–2.69 dB compared with the multi-carrier phase code signal under the typical parameters expressed in this paper.

1. INTRODUCTION

In the aspect of improving the performance of communication system, some research shows that MIMO antenna system [1] has more potential than single input single output (SISO) antenna system. Different from beamforming, MIMO system can make good use of the independence of the signals at the array elements, which is one of the reasons that MIMO radar [2] system has attracted much attention in recent years. It can use orthogonal transmitting waveform to provide additional diversity to detect and estimate targets. In this paper, MIMO radar system is introduced into the anti-ISRJ technology [3]. The simulation results show that MIMO radar has better anti-ISRJ jamming ability.

ISRJ is a kind of jamming type based on digital radio frequency memory (DRFM) [4–6]. Because ISRJ signal is jammer, several coherent false targets will be generated after pulse compression [7–9].

Some conventional radars are mainly suppressed by comparing the difference between the jamming signal in the radar receiver and the echo of the real target. But the anti-ISRJ performance is limited. Chen et al. [10] proposed a filtering method based on stacked bidirectional gated recurrent unit (SBIGRU) and infinite training for the suppression of ISRJ in linear frequency modulation (LFM) pulse compression radar. Zhou et al. [11] proposed an iterative algorithm to optimize waveform and mismatch filter. Ren et al. [12] analyzed the working principle of ISRJ. Li et al. [13] proposed a radar signal based on time-frequency random coding (TFRC). Huan et al. [14] proposed a new ISRJ countermeasure scheme based on Bayesian compressed sensing (BCS). Wei et al. [15] proposed a dynamic electronic countermeasure scheme based on jammer parameter estimation and transmitting

Received 22 September 2021, Accepted 14 April 2022, Scheduled 6 May 2022

* Corresponding author: Wei Wang (wangwei@csust.edu.cn).

¹ College of Computer and Communication Engineering, Changsha University of Science & Technology, Changsha 410000, China. ² College of Electronic Science and Technology, National University of Defense Technology, Changsha 410000, China.

signal design. Zhang et al. [16] proposed an anti-ISRJ method based on stepped linear frequency modulation (LFM) waveform. Liu et al. [17] introduced the structure of ISRJ based on DRFM and verified the feasibility of the structure. Ciunozzo et al. [18] developed sub-optimal fusion rules improved jamming suppression capability. Devaney [19] applied the time reversal imaging method to radar imaging. Ciunozzo et al. [20] studied the performance of multiple signal classification (MUSIC) in computational time-reversal (TR) applications.

Considering the advantages of MIMO technology such as reducing the space complexity, Chahrouh et al. [21] studied the hybrid beamforming of a MIMO radar system in jamming environment. Gui and Wang [22] proposed an optimization method for designing cognitive MIMO radar waveforms under constant modulus and spectral interference constraints to suppress spectral interference. Chernyak [23] proved by simulation that MIMO radar can eliminate mainlobe interference by transmitting multiple different waveforms at any phase without suppressing the signal. Aittomaki and Koivune [24] introduced a mismatched filter design method that minimized interference and jamming power at the filter output. He and Huang [25] proposed a weighted linear self-interference channel estimator.

The above analysis shows that MIMO radar has certain advantages in anti-jamming field. Based on multi-carrier phase code (MCPC) radar signal, this paper proposes a new conception of MIMO radar and designs a signal with anti-ISRJ characteristics, namely RR-MCPC signal. Chaotic binary code is used to encode each chip in time domain, and then the carrier signal is divided into multiple channels to transmit orthogonal carrier signals. Because the multi-waveform signals remain independent in space, the anti-jamming performance of signal is improved in waveform generation phase. On this basis, this paper uses the RR method to counter the ISRJ. Although the addition of redundant coding will cause certain bandwidth losses to the radar signal itself, the simulation shows that the RR-MCPC signal has anti-ISRJ characteristics.

In this paper, based on the time-domain sampling characteristics of intermittent sampling, this paper designs redundant coding in time-domain and frequency-domain, so that the interfering party will surely acquire redundancy. This redundant information cannot be matched with the matched filter of the corresponding channel, so as to improve the signal to interference ratio after information processing.

The remainder of the paper is arranged as follows. Section 2 discusses the principle of intermittent sampling and repeater jamming. Section 3 describes the RR-MCPC signal model. Section 4 shows the MIMO radar model and simulates the ambiguity function of RR-MCPC signal. Section 5 introduces the characteristics of the intermittent sampling and repeater jamming. Section 6 carries out simulation experiments and analysis. Section 6 summarizes the work of this paper.

2. PRINCIPLE OF ISRJ

Compared with the traditional jamming mode, the ISRJ can skillfully use the matched filtering characteristics of pulse compression radar to produce more effective jamming to LFM pulse compression radar. At present, the researches of ISRJ patterns show that the differences of forwarding patterns and parameter settings will cause different jamming effects. The jamming energy is inversely proportional to the number of false targets. Taking typical direct forwarding and repeating forwarding interference patterns as examples, the interference principle is analysed, and the model block diagram is shown in Figure 1.

The jammer repeats the current sampling signal according to the preset number of times after sampling a section of radar transmission signal, and then repeats the current sampling signal after sampling a small section of signal, so as to repeat the above process until the end of the radar signal.

In the international radar conferences from 2003 to 2004, such as the 38th Asilomar conference and the 2004 IEEE radar conference, scholars formally put forward the concept of MIMO radar. Among them, the representative article is "MIMO Radar: An Idea Whose Time Has Come" written by Fishler et al. in 2004 [26]. MIMO radar is divided into distributed MIMO radar and centralized MIMO radar. Distributed layout of transceiver antenna units in distributed MIMO radar brings the multi-angle detection field of view to the target and improves the detectability of the radar to the target. The transceiver antenna units of centralized MIMO radar are close to each other. The angle of view of

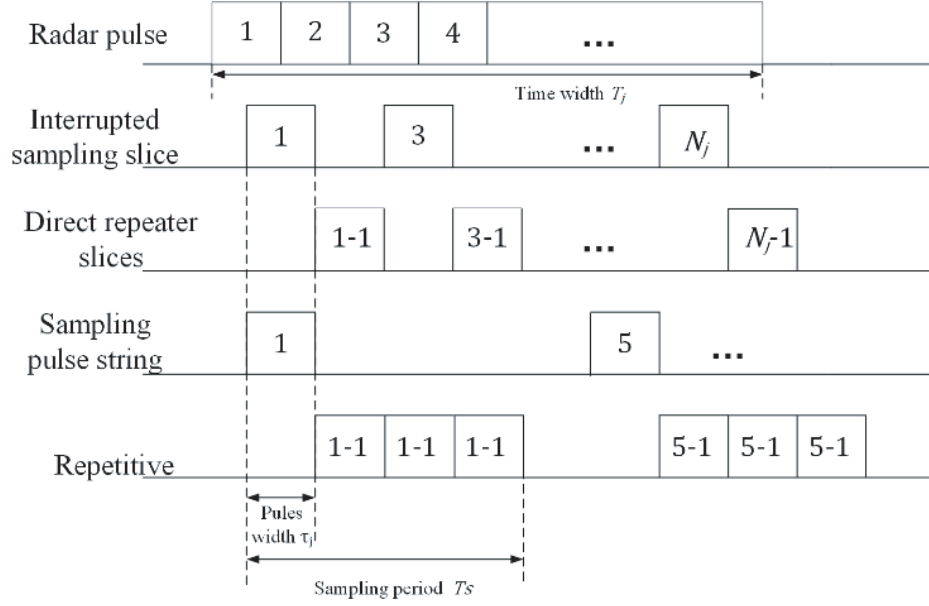


Figure 1. Mechanism of ISJR.

each antenna unit to the target is approximately the same. However, each array element can transmit different signal waveforms. Thus, waveform diversity is obtained.

The interrupt sampling function of repeater jammer based on DRFM can be described as follows:

$$p(t) = \text{rect}\left(\frac{t}{\tau}\right) \otimes \sum_{n=-\infty}^{+\infty} \delta(t - nT_s) \quad (1)$$

where τ and $\text{rect}(t/\tau)$ are the sampling duration and a rectangular envelope pulse with a value of 1 ($0 \leq t \leq \tau$) or 1 (*otherwise*). T is the pulse repetition interval. \otimes is the convolution operation. $D_r = \tau/T_s$ is the duty cycle of the sample.

3. RR-MCPC SIGNAL MODEL

Different from the most popular filter design method at present, RR-MCPC starts from the point of waveform design [27]. RR-MCPC uses chaotic sequence to encode each chip in time domain for signals with a multi-carrier phase code polyphase coding structure. Subcarriers are divided into multiple channels for transmission, and the received signals are processed in each channel. Random redundant processing reduces the coherence between pulse and intra pulse carrier to a certain extent, makes the signal have anti ISRJ characteristics, and can effectively suppress the interference of ISRJ false target.

RR-MCPC signal has several features. It consists of P subcarriers. Each subcarrier contains M -bit phase code, and the width of each phase code chip is the same. In order to guarantee the orthogonality between subcarriers, the number of chips multiplied by the number of carrier waves is equal to the bandwidth multiplied by the time width. The signal of RR-MCPC offers a more agile waveform frame.

The complex envelope $x(t)$ of RR-MCPC signal can be shown as:

$$\begin{aligned} x(t) &= \sum_{p=1}^P \omega_p \exp(j2\pi f_p t) u_p(t) \\ &= \sum_{p=1}^P \sum_{m=1}^M \omega_p \exp(j2\pi f_p t) \varepsilon_{p,m} \times \left\{ 1 - \text{rect} \left[\left(t - R_p \frac{m}{N_{rr}} \right) - (R_p + 1) \frac{m}{N_{rr}} \right] \right\} \end{aligned} \quad (2)$$

where P and M are the number of carriers and the number of coding chips. $\omega_p = |\omega_p|e^{j\phi_p}$, and $|\omega_p|$ is the weighted amplitude on the p th subcarrier. ϕ_p is the weighted phase. $u_p(t)$ and $f_p = (p-1)(1/t_b)$ are the complex envelope of the subcarrier signal and the p th subcarrier frequency. t_b is the duration of a single chip. $\Delta f = 1/t_b$ is the subcarrier frequency interval. $\varepsilon_{p,m}$ is the phase coding of the m th chip on the p th subcarrier. Nrr is the random redundancy parameter. $R_p \in [1, Nrr]$ is $R_1 \neq R_2 \neq \dots \neq R_{\frac{Nrr}{p}}, R_{\frac{Nrr}{p}+1} \neq R_{\frac{Nrr}{p}+2} \neq \dots \neq R_{2 \times \frac{Nrr}{p}}, \dots, R_{(p-1) \times \frac{Nrr}{p}+1} \neq R_{(p-1) \times \frac{Nrr}{p}+2} \neq \dots \neq R_{Nrr}$. The echo signal of scattering target at range R is as follows:

$$x_r(t) = Ax(t - \Delta t) = A \sum_{p=1}^P \sum_{m=1}^M \omega_p a_{p,m} \times \beta_p \text{rect}[t - \Delta t - (m-1)t_b] \exp[j2\pi f_p(t - \Delta t)] \quad (3)$$

where $\Delta t = 2R/c$ is the time delay. A and c are the echo amplitude and propagation velocity. In order to constitute coherent false target interference, the radar signal received by jammer is sampled and stored intermittently by ISRJ method. Assume that R_j is the relative distance between radar and jammer. Interrupt sampling interference signal can be expressed as:

$$x_j(t) = \sum_{n=0}^{N_s} \sum_{p=0}^P \sum_{m=0}^M \omega_p \varepsilon_{p,m} \text{rect}\left[\frac{t - \Delta\tau(n)}{\tau}\right] \times \exp\{j2\pi f_p[t - \Delta\tau(n)]\} \quad (4)$$

where $\Delta\tau(n) = t - 2R_j/c - nT_s - t_0$ and t_0 are the signal processing delay of interference. n is the number of repeats. $n(t)$ is the Gaussian noise. N_s is the upper limit of forwarding times. The whole echo received can be expressed as [28, 29]:

$$x_{echo}(t) = x_r(t) + x_j(t) + n(t) \quad (5)$$

The time-frequency (TF) structure of RR-MCPC signal is manifested in Figure 2.

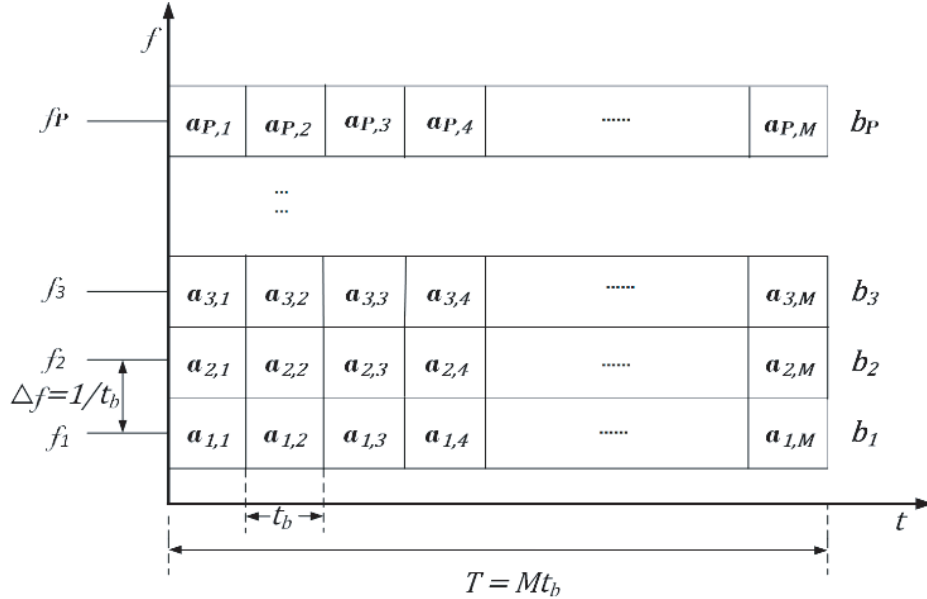


Figure 2. TF framing of RR-MCPC signal.

$B = P * \Delta f$ and $T = M * t_b$ are the signal bandwidth and signal duration. RR-MCPC signal adds a modulation dimension contrast with OFDM signal, which designs the modulation mode more nimbly.

4. MIMO RADAR MODEL

This section mainly discusses and studies the related principle knowledge involved in MIMO radar waveform design. Supposing that MIMO radar has M transmitting antenna and N receiving antenna,

the discrete-time baseband signal transmitted by the M antenna is $x_m(k)$, and θ represents the position parameters of general targets, such as azimuth and range. Then the transmitting signal vector and transmitting steering vector of M transmit antenna are respectively:

$$\begin{cases} x(k) = [x_1(k), x_2(k), \dots, x_m(k)]^T \\ \alpha(\theta) = [e^{-j2\pi f_0 \tau_1(\theta)}, e^{-j2\pi f_0 \tau_2(\theta)}, \dots, e^{-j2\pi f_0 \tau_M(\theta)}]^T \end{cases}$$

Assuming that the transmitted detection signal is the propagation and that narrow band is non-dispersive, the baseband signal at the target location can be expressed as:

$$\sum_{m=1}^M e^{-j2\pi f_0 \tau_m(\theta)} x_m(k) = \mathbf{a}^*(\theta) \mathbf{x}(k), \quad k = 1, 2, \dots, K \quad (6)$$

where f_0 is the radar carrier frequency. τ_m is the time required for the signal to arrive at the target from the m th transmitting antenna. $(\cdot)^*$ is the conjugate transpose, and K is the number of pulse samples of each transmitting signal.

In this paper, the transmitting antenna and receiving antenna of centralized MIMO radar are respectively arranged.

$$x_{echo}(t) = x_r(t) + x_j(t) + n(t) \quad (7)$$

where $x_j(t)$ is the interference signal of interrupt sampling, and $x_r(t)$ is the echo signal.

According to the MIMO characteristics, we set up the MIMO radar waveforms of four transmitting antennas and four receiving antennas, and the MIMO radar waveforms of eight transmitting antennas and eight receiving antennas, hereinafter referred to as $4 * 4$ MIMO and $8 * 8$ MIMO.

In multi-carrier phase code radar signal, each subcarrier can be randomly coded. In this paper, a total of 8 subcarriers are designed, and the subcarriers are divided into two groups for multi-channel transmission. Each signal is sent by 4-channel or 8-channel MIMO channel. On this basis, redundant coding is added, and a part of each signal data is set to zero according to the random arrangement. The time-frequency composition of the signal is shown in Figure 3, and the shaded part is the redundant coding.

The fuzzy function is calculated as follows:

$$\begin{aligned} \chi(\tau, v) &= \int_{-\infty}^{\infty} x(t)x^*(t + \tau) \exp(j2\pi vt) dt \\ &= \sum_{p=1}^P \sum_{l=1}^P \omega_p \omega_l^* \beta_p \beta_l^* \int_{-\infty}^{\infty} u_p(t) u_l^*(t + \tau) \exp(j2\pi f_p t) \times \exp[-j2\pi f_l(t + \tau)] \exp[j2\pi vt] dt \\ &= \sum_{p=1}^P \sum_{l=1}^P \omega_p \omega_l^* \beta_p \beta_l^* \exp[-j2\pi l \Delta f \tau] \int_{-\infty}^{\infty} u_p(t) u_l^*(t + \tau) \exp[(j2\pi(p - l)\Delta f t + j2\pi vt)] dt \\ &= \sum_{p=1}^P \omega_p^2 \beta_p^2 \exp[-j2\pi p \Delta f \tau] \sum_{q=-M}^M \chi_u(\tau - qt_b, v) \sum_{m=1}^{M-|q|} a_{p,m} a_{p,m+q}^* \exp(j2\pi v m t_b) \\ &\quad + \sum_{p=1}^P \sum_{l=1, p \neq l}^P \omega_p \omega_l^* \beta_p \beta_l^* \times \exp[-j2\pi l \Delta f \tau] \sum_{q=i}^{i+1} \chi_u[\tau - qt_b, (p - l)\Delta f + v] \\ &\quad \cdot \sum_{m=1}^M a_{p,m} a_{l,m+q}^* \exp(j2\pi v m t_b) \end{aligned} \quad (8)$$

$$\chi_u(\tau, v) = \begin{cases} \exp[j\pi v(t_b - \tau)] \frac{\sin(\pi v(t_b - |\tau|))}{\pi v(t_b - |\tau|)} \left(1 - \frac{|\tau|}{t_b}\right) & |\tau| \leq t_b \\ 0, & |\tau| > t_b \end{cases} \quad (9)$$

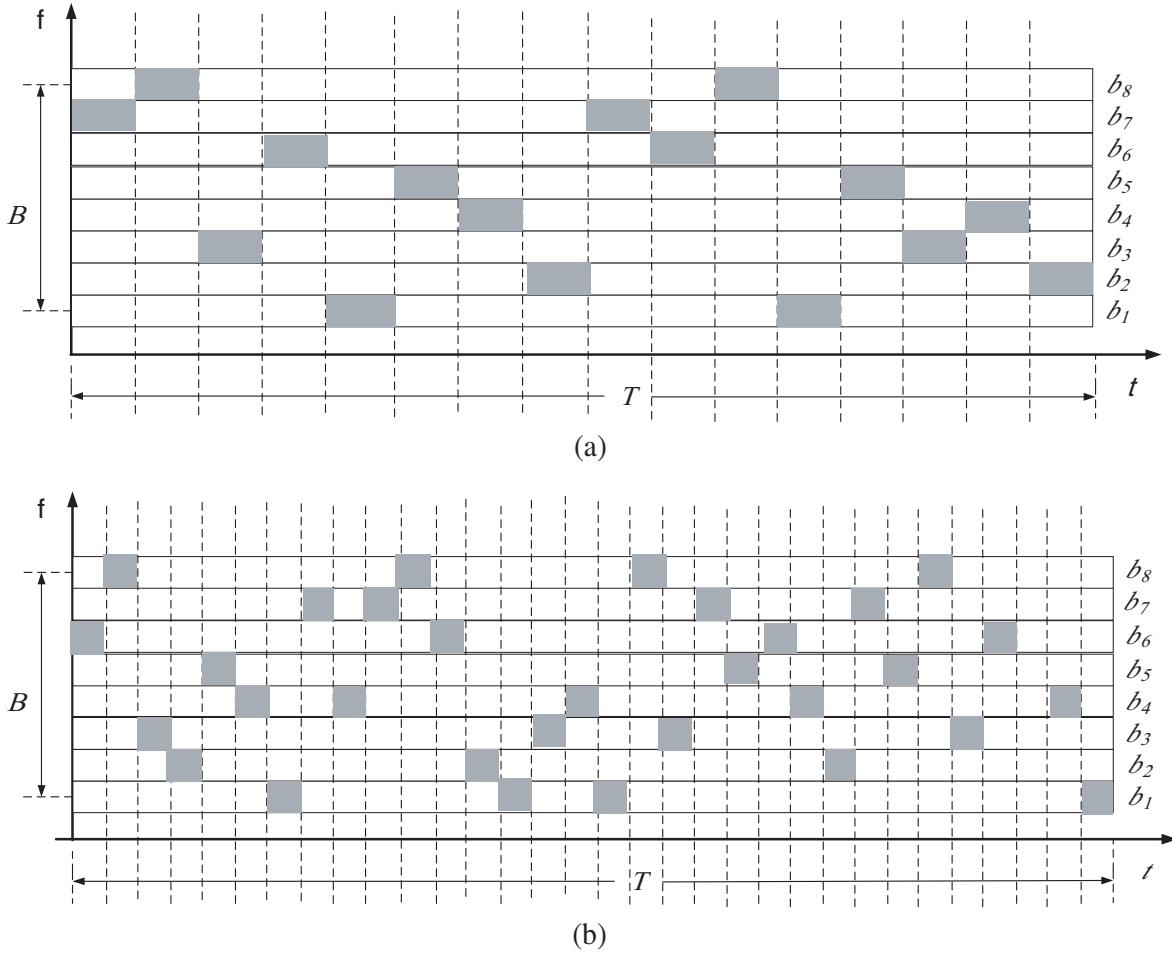


Figure 3. (a) RR-MCPC signal ($Nrr = 16$). (b) RR-MCPC signal ($Nrr = 32$).

$u(t)$ rectangular window function is the fuzzy function of $\chi_u(\tau, v)$.

Under the same time bandwidth, taking 4×4 MIMO as an example, we simulated the ambiguity function of RR-MCPC signal under $Nrr = 16$ and $Nrr = 32$ and compared it with LFM signal, as shown in Figure 4.

As can be seen from Figures 4(a) (b), the ambiguity function diagram of RR-MCPC signal is pushpin type, and the central peak surrounds a large number of envelopes. Figure 4(c) shows that the LFM signal has oblique edge ambiguity.

Comparing the two-dimensional ambiguity maps of the three signals, their resolutions in time domain and frequency domain are basically the same, and the main lobe peaks are also the same, both of which are 42.14. The main lobe width of RR-MCPC ($Nrr = 16$) signal is $2.4 \times 10^6 - 8$. The signal main lobe width of RR-MCPC ($Nrr = 32$) is $2.4 \times 10^6 - 8$. The main lobe width of LFM signal is $1.2 \times 10^6 - 8$. By comparison, the main lobe width of LFM signal is the narrowest. So the resolution of LFM signal is the highest. When the sidelobe peak of LFM signal is 28.14, the sidelobe peak of RR-MCPC ($Nrr = 16$) signal is 26.98, and the sidelobe peak of RR-MCPC ($Nrr = 32$) signal is 26.22. It is less than the sidelobe peak of LFM signal. Therefore, the resolution of RR-MCPC signal is slightly better than that of LFM signal. Compared with the bevel ambiguity function, the pushpin ambiguity function does not have the characteristics of range Doppler coupling and low side lobe. Therefore, RR-MCPC signal has better target detection ability than LFM signal.

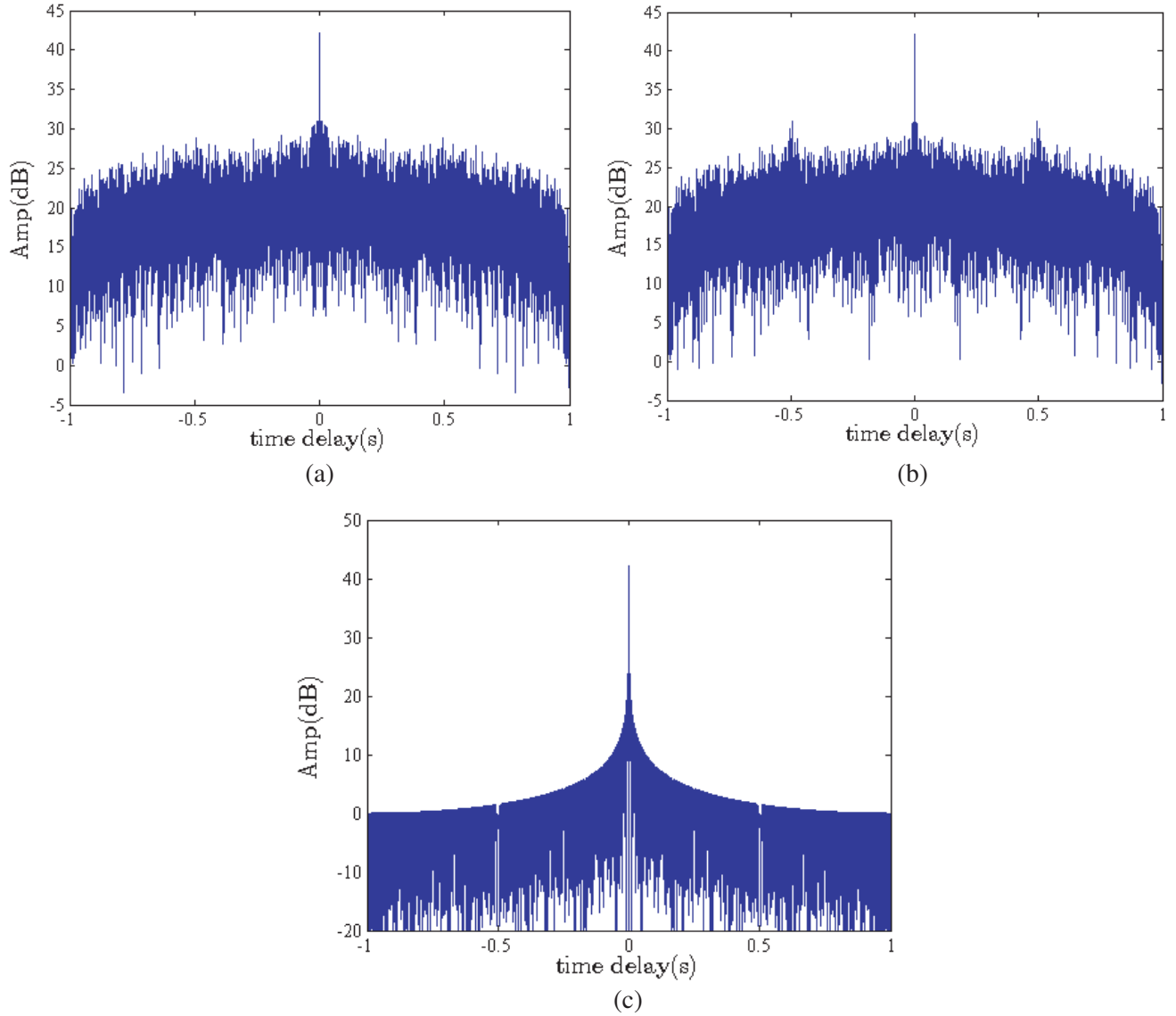


Figure 4. Doppler axial blur. (a) RR-MCPC ($N_{rr} = 16$). (b) RR-MCPC ($N_{rr} = 32$). (c) LFM.

5. JAMMING SUPPRESSION

From the point of waveform design, this paper designs an RR-MCPC signal waveform. For signals with a multi-carrier phase code polyphase coding structure, chaotic sequences are used to encode each chip in time domain. Subcarriers are divided into multiple channels for transmission, and the received signals are processed in each channel. Random redundancy processing ensures that no matter how intermittent sampling is in the time domain, redundant information will be sampled on a certain channel. Thus, it is mismatched with the matched filter. Make the ISRJ signal resistant.

The radar echo signal can be obtained by short-time Fourier transform (STFT) transformation:

$$S_m(t, f) = \int_{-\infty}^{\infty} x(\tau)\omega(\tau - t) \exp(-j2\pi f\tau) d\tau \quad (10)$$

The normalized filter $H(f)$ can be expressed as:

$$H(f) = |S_m(t, f)|^2 \quad (11)$$

The output of pulse pressure is as follows:

$$P(f) = H(f) \times \int S_m(t) \exp(-j2\pi ft) dt \quad (12)$$

In this paper, SJR improvement factor is used to evaluate the performance of interference suppression. It can be expressed as:

$$\delta_{SJR} = SJR_{PC} - SJR \quad (13)$$

where SJR_{PC} is the SJR value after pulse compression.

6. SIMULATION ANALYSIS

In this part, we use chaotic binary phase coding with good pseudo-random. Therefore, the sampling period is set to the integer times of the width of the sampling pulse. The simulation parameters are designed as manifested in Table 1.

Table 1. Simulation parameters.

Parameter	Value
Timewidth (TW)	0.125 μ s
Number of subcarriers	8
Number of chips	1024
SNR	-20 ~ 20 dB
Bandwidth (BW)	64 MHz

In this section, the multi-carrier phase code signal and the RR-MCPC signal proposed in this paper are used to simulate ISRJ. The results are manifested in Figure 5.

It can be known that a single false target ahead of the true target will be generated in each experiment. Normalizing the data, the ISRJ simulation results of 4×4 MIMO's multi-carrier phase code signal and RR-MCPC signal are respectively manifested in Figure 5. In Figure 5(a), there is a false

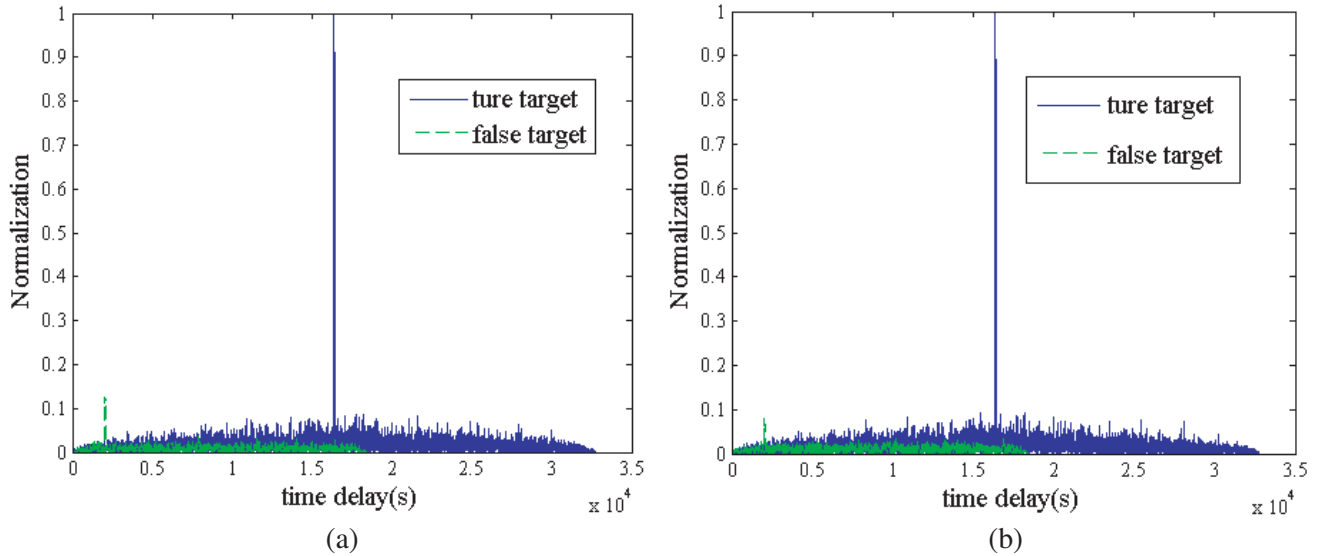


Figure 5. Comparison of 4×4 MIMO interference suppression results. (a) MCPC signal Anti ISRJ. (b) RR-MCPC ($N_{rr} = 16$) signal anti ISRJ.

target with an amplitude of 0.12. However, in Figure 5(b), the amplitude of the false target is reduced to 0.08, and the ISRJ experimental results on RR-MCPC show that the interference and harmonic interference are obviously suppressed.

This section analyses the anti-interference effects of multi-carrier phase code and RR-MCPC ($N_{rr} = 16$) of 4×4 MIMO under different SNR conditions.

The experimental results are manifested in Figure 6.

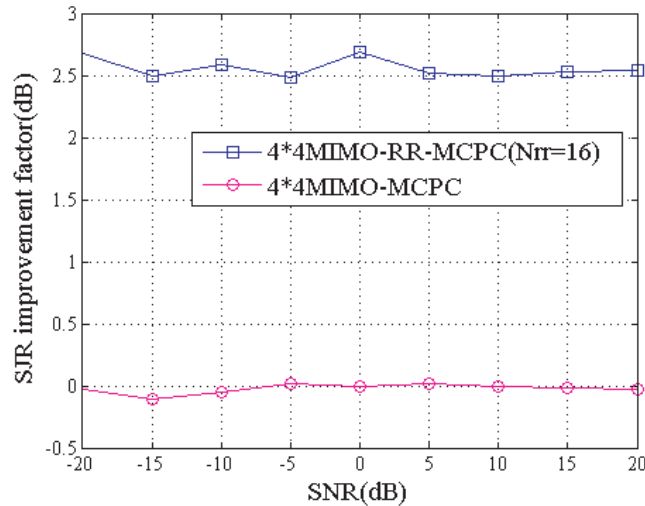


Figure 6. Interference suppression performance under different SNR conditions.

It can be seen from Figure 6 that the SJR improvement factor of the RR-MCPC signal proposed in this paper is 2.47–2.69 dB higher than that of the multi-carrier phase code signal under different signal-to-noise ratios at 4×4 MIMO. Compared with [13], the effect of this paper is better. RR-MCPC signal is planned beforehand. The waveform design is easy to implement in signal processing. This method can be combined with the existing anti-ISRJ methods.

7. CONCLUSION

According to the principle of ISRJ discontinuous sampling in time domain, an anti-ISRJ method of RR-MCPC signal based on MIMO radar is proposed in this paper. The multi-carrier phase code signal is coded in time domain by chaotic sequence with good pseudo randomness. In addition, a part of signal chips are randomly arranged in time domain and frequency domain, and the amount of redundant coding is equal. In MIMO radar, the subcarriers of radar signal are divided into multiple channels for transmission, and then the received signal is processed in each channel. The simulation results show that RR-MCPC signal has a certain efficiency to inhibit ISRJ signal. This paper provides a new solution to the problem of radar anti-jamming by designing the waveform.

In the next step, further research and semi-physical test will be carried out to verify the anti-interference effect of the waveform designed in this paper in complex electromagnetic environment.

ACKNOWLEDGMENT

This work was supported in part by the Changsha Natural Science Foundation kq2014111, and Seed fund of multi-sensor intelligent detection and identification technology R & D Center ZZJJ202103-02.

REFERENCES

1. Majd, M. N., M. Radmard, M. M. Chitgarha, et al., “Diversity-multiplexing tradeoff in MIMO radars,” *IET Radar, Sonar & Navigation*, Vol. 11, No. 4, 691–700, 2017.

2. Xiong, J., W. Q. Wang, C. Cui, et al., "Cognitive FDA-MIMO radar for LPI transmit beamforming," *IET Radar, Sonar & Navigation*, Vol. 11, No. 10, 1574–1580, 2017.
3. Feng, D. J., H. M. Tao, Y. Yang, et al., "Jamming de-chirping radar using interrupted-sampling repeater," *Science China Information Sciences*, Vol. 54, No. 10, 2138–2146, 2011.
4. Lu, Y. and S. Li, "CFAR detection of DRFM deception jamming based on singular spectrum analysis," *2017 IEEE International Conference on Signal Processing, Communications and Computing (ICSPCC)*, 1–6, Xiamen, China, 2017.
5. Zhou, C., Q. Liu, et al., "Parameter estimation and suppression for DRFM-based interrupted sampling repeater jammer," *IET Radar, Sonar & Navigation*, 56–63, 2018.
6. Hao, H., M. Pan, S. Gong, et al., "Estimating and calibrating the response of multiple wideband digital radio frequency memories in a hardware-in-the-loop system using shuffled frog leaping algorithm," *IET Radar, Sonar & Navigation*, Vol. 10, No. 5, 827–833, 2016.
7. Zhong, S., X. Huang, H. Wang, et al., "Anti-intermittent sampling repeater jamming waveform design based on immune genetics," *2019 IEEE International Conference on Power, Intelligent Computing and Systems (ICPICS)*, 553–559, Shenyang, China, 2019.
8. Zhou, C., Z. Tang, Z. Zhu, et al., "Anti-interrupted sampling repeater jamming waveform design method," *Dianzi Yu Xinxi Xuebao/Journal of Electronics and Information Technology*, Vol. 40, No. 9, 2198–2205, 2018.
9. Yu, M., S. Dong, X. Duan, et al., "A novel interference suppression method for interrupted sampling repeater jamming based on singular spectrum entropy function," *Sensors*, Vol. 19, No. 1, 136–157, 2019.
10. Chen, J., S. Xu, J. Zou, et al., "Interrupted-sampling repeater jamming suppression based on stacked bidirectional gated recurrent unit network and infinite training," *IEEE Access*, 107428–107437, 2019.
11. Zhou, K., D. Li, Y. Su, et al., "Joint design of transmit waveform and mismatch filter in the presence of interrupted sampling repeater jamming," *IEEE Signal Processing Letters*, Vol. 27, 1610–1614, 2020.
12. Ren, Z., M. Jiang, and L. Zhang, "Orthogonal phase-frequency coded signal in a pulse against interrupted sampling repeater jamming," *The Journal of Engineering*, 7573–7576, 2019.
13. Li, J., X. Luo, X. Duan, et al., "A novel radar waveform design for anti-interrupted sampling repeater jamming via time-frequency random coded method," *Progress In Electromagnetics Research M*, Vol. 98, 89–99, 2020.
14. Huan, S., G. Dai, G. Luo, et al., "Bayesian compress sensing based countermeasure scheme against the interrupted sampling repeater jamming," *Sensors*, Vol. 19, No. 15, 3279–3285, 2019.
15. Wei, Z., L. Zhen, B. Peng, et al., "ECCM scheme against interrupted sampling repeater jammer based on parameter-adjusted waveform design," *Sensors*, Vol. 18, No. 4, 1141–1157, 2018.
16. Zhang, J., M. U. Huqiang, S. Wen, et al., "Anti interrupted-sampling repeater jamming method based on stepped LFM waveform," *Systems Engineering and Electronics*, 2019.
17. Liu, Q. L., Z. Liu, Qi-Xiang F.U., et al., "A DRFM-based repeater jammer with interrupted sampling," *Radar & Ecm*, 2007.
18. Ciunzo, D., A. Aubry, and V. Carotenuto, "Rician MIMO channel- and jamming-aware decision fusion," *IEEE Transactions on Signal Processing*, Vol. 65, No. 99, 3866–3880, 2017.
19. Devaney, A. J., "Time reversal imaging of obscured targets from multistatic data," *IEEE Transactions on Antennas & Propagation*, Vol. 53, No. 5, 1600–1610, 2005.
20. Ciunzo, D., G. Romano, and R. Solimene, "Performance analysis of time-reversal MUSIC," *IEEE Transactions on Signal Processing*, Vol. 63, No. 10, 2650–2662, 2015.
21. Chahrour, H., S. Rajan, R. Dansereau, et al., "Hybrid beamforming for interference mitigation in MIMO radar," *2018 IEEE Radar Conference (Radar Conf. 18)*, 1005–1009, IEEE, Oklahoma City, OK, USA, 2018.

22. Gui, R. and W. Q. Wang, "Constant modulus waveforms with restraining spectral interferences for cognitive MIMO radar," *2017 IEEE Radar Conference (Radar Conf. 17)*, 0335–0339, IEEE, Seattle, WA, USA, 2017.
23. Chernyak, V., "On signal detection with mainlobe cancellation interference in Multisite Radar Systems and MIMO radars," *2015 European Radar Conference (EuRAD)*, 137–140, Paris, France, 2015.
24. Aittomaki, T. and V. Koivunen, "Mismatched filter design and interference mitigation for MIMO radars," *IEEE Transactions on Signal Processing*, Vol. 65, No. 2, 454–466, 2017.
25. He, M. and C. Huang, "Self-interference cancellation for full-duplex massive MIMO OFDM with single RF chain," *IEEE Wireless Communication Letters*, Vol. 99, 26–29, 2019.
26. Fishler, E., A. Haimovich, R. Blum, D. Chizhik, L. Cimini, and R. Valenzuela, "MIMO radar: an idea whose time has come," *Proceedings of the 2004 IEEE Radar Conference (IEEE Cat. No.04CH37509)*, 71–78, April 2004. doi: 10.1109/NRC.2004.1316398.
27. Tang, L., Y. Zhu, and Q. Fu, "Designing waveform sets with good correlation and stopband properties for MIMO radar via the gradient-based method," *Sensors*, 999–1020, 2017.
28. Deng, H., "Polyphase code design for orthogonal netted radar systems," *IEEE Trans. Signal Process.*, Vol. 52, 3126–3135, 2004.
29. Yang, Y., R. S. Blum, and Z. S. He, "MIMO radar waveform design via alternating projection," *IEEE Trans. Signal Process.*, Vol. 58, 1440–1445, 2010.